

# The protective effect of LCZ696 in coxsackievirus B3-induced acute viral myocarditis mice

Xu Jing<sup>1†</sup>, Lian Hao<sup>2†</sup>, Lin Yuan-Nan<sup>1†</sup>, Liu Wei-Ke<sup>1</sup>, Jin Lu-Shen<sup>1</sup>, Ke Jin-Yan<sup>1</sup>, Chen Yi-Lian<sup>1</sup>, Qiu Yi-Xuan<sup>1</sup>, Ge Li-Sha<sup>3\*</sup> and Li Yue-Chun<sup>1\*</sup>

<sup>1</sup>Department of Cardiology, Second Affiliated Hospital and Yuying Children's Hospital of Wenzhou Medical University, Wenzhou, 325000, China; <sup>2</sup>Department of Cardiology, The first people's Hospital of Wenling, Wenling, China; and <sup>3</sup>Department of Pediatric Emergency, The Second Affiliated Hospital and Yuying Children's Hospital of Wenzhou Medical University, Wenzhou, China

## Abstract

**Aims** Acute viral myocarditis (AVMC) is the aetiology of heart failure (HF) with few specific treatments. The improvement of left ventricular ejection fraction (LVEF) is a critical predictor for the prognosis of AVMC. LCZ696 is a drug used in HF to improve LVEF, with a few research on AVMC. In this research, we evaluated the effects and mechanism of LCZ696 in improving LVEF in AVMC.

**Methods** Eighty 4-week-old male BALB/c mice were randomly divided into four groups of 20: Sham; Sham + LCZ696 (60 mg/kg/d); AVMC; AVMC + LCZ696. The above experiments were repeated by CVB3-infected HL-1 and Mdivi-1 to down-regulated dynamin-related protein 1(Drp1). Adeno-associated virus 9 (AAV9) with enhanced green fluorescent proteins (GFP) was injected to produce Drp1-overexpression mice and set up four groups: AVMC group, AVMC + AAV group, AVMC + LCZ696 group, and AVMC + LCZ696 + AAV group ( $n = 20$  in each group). LVEF was evaluated by echocardiography at a similar heart rate (HR) at d7, Drp1 (p-Drp1), inflammation and apoptosis by histology and Western blot (WB), and mitochondrial by electron microscopy.

**Results** Cardiac function were injured in AVMC that LCZ696 reversed (LVEF, %: Sham:  $68.99 \pm 9.67$ ; Sham + LCZ696:  $71.96 \pm 6.20$ ; AVMC:  $30.95 \pm 6.40^*$ ; AVMC + LCZ696:  $68.99 \pm 9.67^{*#}$ ,  $*P < 0.05$  vs. Sham,  $\#P < 0.05$  vs. AVMC). LCZ696 attenuated p-Drp1 expression, inflammation, apoptosis, and mitochondrial fission (p-Drp1/Drp1: Sham: 1; Sham + LCZ696:  $1.37 \pm 0.22$ ; AVMC:  $2.29 \pm 0.36^*$ ; AVMC+LCZ696:  $1.43 \pm 0.08^{*#}$ ,  $*P < 0.05$  vs. Sham,  $\#P < 0.05$  vs. AVMC). Some of the above results were repeated in CVB3-infected HL-1 cells and Mdivi-1. AAV increased Drp1 expression and mitochondrial fission, inflammatory, and apoptosis. Compared with the AVMC + AAV group, the LVEF increased from  $24.44 \pm 0.03\%$  to  $32.33 \pm 0.05\%$  in the AVMC + LCZ696 + AAV group ( $P < 0.05$ ), p-Drp1/Drp1 decreased from  $0.54 \pm 0.12$  to  $0.42 \pm 0.09^*$ , and IL-6, c-IL-1 $\beta$ , and c-caspase-3/caspase-3 decreased from  $1.07 \pm 0.22$  to  $0.72 \pm 0.08^*$ , from  $1.03 \pm 0.14$  to  $0.79 \pm 0.09^*$ , and from  $4.69 \pm 0.29$  to  $0.92 \pm 0.13^*$ , respectively ( $*P < 0.05$ ).

**Conclusions** LCZ696 has a protective effect on AVMC by improving LVEF and reducing inflammation and apoptosis, which may be due to the inhibition of Drp1-mediated mitochondrial fission.

**Keywords** LCZ696; AVMC; LVEF; Drp1; Inflammation; Apoptosis

Received: 27 October 2021; Revised: 17 August 2022; Accepted: 2 October 2022

\*Correspondence to: Li Yue-Chun, Department of Cardiology, Second Affiliated Hospital and Yuying Children's Hospital of Wenzhou Medical University, Wenzhou 325000, China. Email [liyuechun1980@sina.com](mailto:liyuechun1980@sina.com)

Ge Li-Sha, Department of Pediatric Emergency, The Second Affiliated Hospital and Yuying Children's Hospital of Wenzhou Medical University, 109 XueYuan Road, Wenzhou Zhejiang, China, Phone: +86-0577-88002216; Fax: +86-0577-88832693. Email: [105247441@qq.com](mailto:105247441@qq.com)

†Contributed equally to the paper.

## Introduction

Acute viral myocarditis (AVMC) is an inflammatory disease associated with substantial mortality and an aetiology for

HF.<sup>1</sup> It generally takes less than one month from the onset of symptoms to a definitive diagnosis of AVMC.<sup>2</sup> According to the latest ESC guidance, myocarditis is defined as a clinical presentation with positive mandatory diagnostic tests

(including electrocardiogram, laboratory tests, echocardiography, and cardiac magnetic resonance) for more than one condition in the absence of significant coronary, valvular, or congenital heart disease or other causes.<sup>1</sup> Endomyocardial biopsy is the diagnostic gold standard of AVMC, with the PCR testing for detecting viruses.<sup>1–3</sup> Echocardiography is partly standard evaluation of patients with a suspected acute cardiac condition; the presence of increased wall thickness and mild segmental hypokinesia may suggest AVMC.<sup>2</sup> LVEF is a sensitive indicator of AVMC progression and treatment outcome and is a criterion for judging the prognosis of AVMC.<sup>1</sup> AVMC is associated with a poor prognosis when complicated by LV dysfunction and HF, which means that the improvement of LVEF is essential for treatment in AVMC.<sup>4,5</sup>

LCZ696, a first-in-class angiotensin receptor-neprilysin inhibitor (ARNI), is composed of the molecular components of ARB valsartan and the neprilysin inhibitor sacbutril.<sup>6</sup> The study reported that LCZ696 reduced mortality and HF events and improved LVEF in HF with reduced ejection fraction (HFrEF).<sup>7</sup> LCZ696 is recommended as a class IB drug to replace ACE-I for HFrEF in 2021 ESC guidelines.<sup>1</sup> It also shows beneficial effects in cardiomyopathy and other cardiovascular diseases, improving cardiac function, reduced peri-infarction, and distal myocardial remodelling as well as fibrosis in infarcted rats.<sup>8–10</sup> The same effects were observed in adriamycin-induced dilated cardiomyopathy (DCM), which also inhibited early myocardial inflammation and apoptosis by alleviating Drp1-mediated mitochondrial dysfunction.<sup>9</sup> In rat with pressure overloaded hearts and dogs with experimental cardiorenal syndrome,<sup>11</sup> LCZ696 protected ventricular myocytes from mitochondrial dysfunction.<sup>12</sup> Although the role of LCZ696 in a subset of cardiovascular diseases has been shown to be mitochondrial related, its effect and the molecular mechanism in AVMC have not been reported.

Mitochondrial fission is an essential part of mitochondrial dynamics, which has been implicated in cardiovascular disease.<sup>13,14</sup> As a key protein in mitochondrial fission, the expression and phosphorylation of Drp1 are associated with mitochondrial function and cellular function, including energy metabolism, apoptosis, and inflammation, as demonstrated in HF, DCM, and septic cardiomyopathy.<sup>15–17</sup> Activating at serine 616 (Ser616) and Ser637 are the two phosphorylation sites of Drp1 that play completely opposite roles. P-Drp1 (Ser616) translocates to the outer membrane and induces mitochondrial fission, whereas Ser637 reverses.<sup>18</sup> Drp1 is associated with AVMC with expression and phosphorylation affecting AVMC inflammation and apoptosis in cardiomyocytes.<sup>19,20</sup> However, it is uncertain whether LCZ696 can achieve therapeutic effects on AVMC by regulating the expression and phosphorylation of Drp1. Therefore, we hypothesized that LCZ696 is effective against AVMC, evaluated the role and specific mechanism, and explored the associations between LCZ696 and Drp1.

## Methods

### Animal care

The investigation conforms to the Guide for the Care and Use of Laboratory Animals published by the US National Institutes of Health (NIH Publication No. 85-23, revised 1985); all experiments were carried out by China Animal Welfare Legislation and were approved by the Wenzhou Medical University Committee on Ethics in the Care and Use of Laboratory Animals. All experimental animals were sacrificed with an overdose of pentobarbital (100 mg/kg, one dose intraperitoneally).

### AVMC and LCZ696

CVB3 (Nancy strain, USA) was maintained and expanded with Hep2 cells. Viral titres were determined by 50% tissue culture infectious dose (TCID<sub>50</sub>). Eighty BALB/c mice were randomly divided into four groups of 20: Sham; Sham + LCZ696; AVMC; AVMC + LCZ696. The AVMC mice were injected intraperitoneally (i.p.) with 0.1 mL CVB3 (10<sup>5</sup> TCID<sub>50</sub>), whereas others were injected with 0.1 mL saline. The day of virus inoculation was defined as Day 0 (d0). LCZ696 (MCE, USA, 60 mg/kg/d) was administered from d1 to d7,<sup>8</sup> the same volume of saline as control. The survival rate in each group will be counted.

### Cell culture and Mdivi-1

HL-1, a cardiac muscle cell line (Beijing Biotechnology Research Institute, China), was kept at 37°C with 5%CO<sub>2</sub>. DMEM medium was supplemented with 10% foetal bovine serum (FBS; DMEM, FBS; Gibco, China). Upon reaching the appropriate confluence, cells were passaged to six-well flat-bottom culture plates and confocal petri dish (Corning, USA) at 8 × 10<sup>5</sup>/well. Cells were divided into four groups: Sham; Sham + Mdivi-1; CVB3; CVB3 + Mdivi-1 (*n* = 6 in each group). Cells were treated with Mdivi-1 (50 μM/mL, MCE, USA) for 40 min before CVB3 addition (MOI = 100) and collected for WB and Hoechst after 24 h.

### Doppler echocardiography study and HR

Echocardiography and HR were obtained by Doppler echocardiography machine (40 MHz phased-array transducer, Vevo 1100, Canada). In blinded fashion, transthoracic echocardiography was performed by an experienced technician the groups on d7 by an M-mode transducer. Mice were treated with isoflurane (1%) delivered by a vaporizer in a mixture of 21% oxygen and 79% nitrogen. After anaesthesia, the chest

shaved, and physiological body temperature was maintained at 37°C. The HR was collected through electrodes. At similar HR levels, long-axis views of M-model were obtained at the papillary muscle level and then the diastolic and systolic LV internal diameters (LVIDd and LVIDs) were measured. The LVEF is then calculated according to the formula in the article by Zacchigna *et al.*<sup>21</sup>

### MitoTracker Red CMXRos

In confocal culture dishes, cell cultures were removed after 24 h and stained with MitoTracker Red CMXRos (YEASEN, 40740ES50, China). The staining working solution was obtained by diluting the storage solution with the cell culture solution to 200 nM and pre-warmed at 37°C for 40 min. After staining, the above staining solution was replaced with a fresh culture medium, and the confocal dish was placed under a fluorescence microscope for observation.

### Hoechst staining

Typical morphological characteristics of apoptotic cells were assessed by Hoechst staining (Beyotime Institute of Biotechnology, China). Cells were fixed with freshly prepared 4% paraformaldehyde, incubated at 5 µg/mL of Hoechst for 15 min at 37°C in the dark, and identified by fluorescence microscopy (Nikon, Tokyo, Japan). Cells were washed twice (5 min each) with PBS before all manipulations. Normal cells showed uniform blue chromatin and organized structures, and the apoptotic cells showed bright blue chromatin that was highly condensed or broken.

### AAV

Recombinant Drp1-overexpressing AAV and negative control AAV (Hanbio Biotech, Shanghai, China) that both contain GFP were prepared and titrated to 10<sup>12</sup> V.G/mL. AAV9 was chosen to electively infect the heart. Eighty BALB/c mice were randomly divided into AVMC; AVMC + AAV; AVMC + LCZ696; and AVMC + LCZ696 + AAV (*n* = 20 in each group). AAV9 (10<sup>11</sup> V.G) was injected in the caudal lateral vein at 2 weeks of age.

### Histopathology and TUNEL assay

Heart was embedded in paraffin and OCT. Samples were sectioned into 5-µm-thick slices and subjected to haematoxylin and eosin (HE) staining or immunohistochemistry (IHC) as previously.<sup>22</sup> Rabbit anti-p-Drp1 antibody (1:200; CST, #3455) and rabbit anti-Drp1 antibody (1:200; CST, #8570)

were used to stain in IHC for 1 h at 37°C; add HRP-polymer conjugate and incubate for 10 min; then add DAB colour solution. The *in situ* cell death assay kit POD (Roche, Germany) for DNA chromatin morphological characterization was used for quantitative detection. Our procedure was performed according to the manufacturer's guidelines. All steps were stored in a lightproof wet box, making sure that the specimen surface was moist. For observation, a microscope with a filter was used for observation and photography. All stained sections were observed using a fluorescence microscope (Olympus, Tokyo, Japan). Three fields were randomly selected for observation and examined in a blinded manner.

### WB

Proteins were extracted from heart tissue and HL-1 cells; the method of WB has been addressed previously.<sup>22</sup> Our antibodies include rabbit anti-Drp1 antibody (1:1000), rabbit anti-p-Drp1 antibody (1:1000), rabbit anti-caspase-3 antibody (1:1000; CST, #9662), rabbit anti-cleaved caspase-3 antibody (c-caspase-3) (1:1000; CST, #9664), rabbit anti-cleaved IL-1β antibody (c-IL-1β) (1:1000; CST, #52718), rabbit anti-IL-6 antibody (1:1000; Abcam, ab208113), rabbit anti-GAPDH antibody (1:1000; CST, #5174), and HRP conjugated goat anti-mouse/anti-rabbit secondary antibody (1:1000; Biosharp, BL001A/BL003A).

### Electron microscopy examination

The apical myocardium was harvested for ultrastructural analysis to quantify mitochondrial fission, and the organization was handled as well as the pictures were taken as in our previous reports.<sup>23</sup>

### Statistical methods

Statistical analysis was performed using SPSS 22 software (Unicom, Mission Hills, CA). A *P* value of less than 0.05 is considered significant. The data are expressed in the form of mean ± standard deviation. Measurement data need to be tested for normality and homogeneity of variance on the data. Shapiro–Wilk test and Kolmogorov–Smirnov test can be used. Subsequent comparisons between multiple groups used one-way ANOVA, and Dunnett's multiple comparisons were used for pairwise comparisons between groups. Count data were compared using the chi-square test or Kruskal–Wallis *H* test.

## Results

### LCZ696 improves survival rates and cardiac function

HR was controlled at similar levels in all mice before cardiac echograms were obtained. The HR in the Sham and Sham + LCZ696 groups were  $556.22 \pm 24.58$  and  $534.00 \pm 19.62$  beats per minute (bpm) ( $P > 0.05$ ),  $451.67 \pm 31.01$  and  $444.33 \pm 26.32$  bpm in AVMC, and AVMC + LCZ696 groups ( $P > 0.05$ ). Like previous experiment, the HR was slower in AVMC ( $P < 0.05$ ). The LVIDd, LVIDs, and LVEF in Sham, Sham + LCZ696, AVMC, and AVMC + LCZ696 groups were  $2.52 \pm 0.24$ ,  $2.61 \pm 0.18$ ,  $3.66 \pm 0.29^*$ ,  $3.09 \pm 0.12$  mm<sup>#</sup>, and  $1.37 \pm 0.16$ ,  $1.33 \pm 0.19$ ,  $2.94 \pm 0.15^*$ ,  $2.22 \pm 0.15$  mm<sup>#</sup>, and  $77.95 \pm 6.79$ ,  $81.49 \pm 6.38$ ,  $39.87 \pm 11.35^*$ ,  $55.36 \pm 6.51\%^*$ , respectively (\* vs. Sham,  $P < 0.05$ ; # vs. AVMC,  $P < 0.05$ ) (Figure 1A). The survival rate of the Sham, Sham + LCZ696, AVMC, and AVMC + LCZ696 group was 100, 100, 56, and 85%, respectively (Figure 1B).

### Anti-inflammatory and anti-apoptotic effect of LCZ696

HE revealed that numerous inflammatory cells infiltrate in the myocardium with myocardial cell fragmentation and disorganization in the AVMC group, which LCZ696 alleviated. No inflammatory cell was observed in the Sham and Sham + LCZ696 groups (Figure 2A). The IHC showed the high expression of inflammatory factor, IL-6, in the AVMC group, which down-regulated by LCZ696, with few expressions in the Sham and Sham + LCZ696 groups (Figure 2B). C-IL-1 $\beta$  and IL-6 in the AVMC group were increased 1.94-fold and 3.64-fold compared with the Sham group ( $P < 0.05$ ) and 1.36-fold and 1.86-fold compared with the AVMC + LCZ696 group ( $P < 0.05$ ). No difference was found between the Sham and Sham + LCZ696 group ( $P > 0.05$ ) (Figure 2D).

More TUNEL-positive cells and higher c-caspase-3/caspase-3 ratio were in the AVMC group, which alleviated by LCZ696 ( $2.91 \pm 0.75$  vs.  $1.64 \pm 0.30$ ,  $P < 0.05$ ), whereas few apoptosis cell in the Sham and Sham + LCZ696 groups (Figure 2C and 2D). No difference of c-caspase-3/caspase-3 ratio was found between Sham and Sham + LCZ696 groups ( $P > 0.05$ ).

### Role of LCZ696 in mitochondria and Drp1

More regular mitochondrial morphology was in the Sham and Sham + LCZ696 groups, while it disordered in the AVMC group with decreased length. After LCZ696 treatment, mito-

chondrial morphology was reversed (Figure 3A). The expression of p-Drp1 in the Sham group was similar to the Sham + LCZ696 group ( $1$  vs.  $1.19 \pm 0.13$ ,  $P > 0.05$ ) and lower than the AVMC group ( $2.29 \pm 0.36$ ,  $P < 0.05$ ). And it was higher in the AVMC group than the AVMC + LCZ696 group ( $1.48 \pm 0.10$ ,  $P < 0.05$ ) (Figure 3B), which the figure of IHC in Figure 3C supported.

### Mdivi-1 inhibit Drp1 expression, inflammatory, and anti-apoptotic level in HL-1

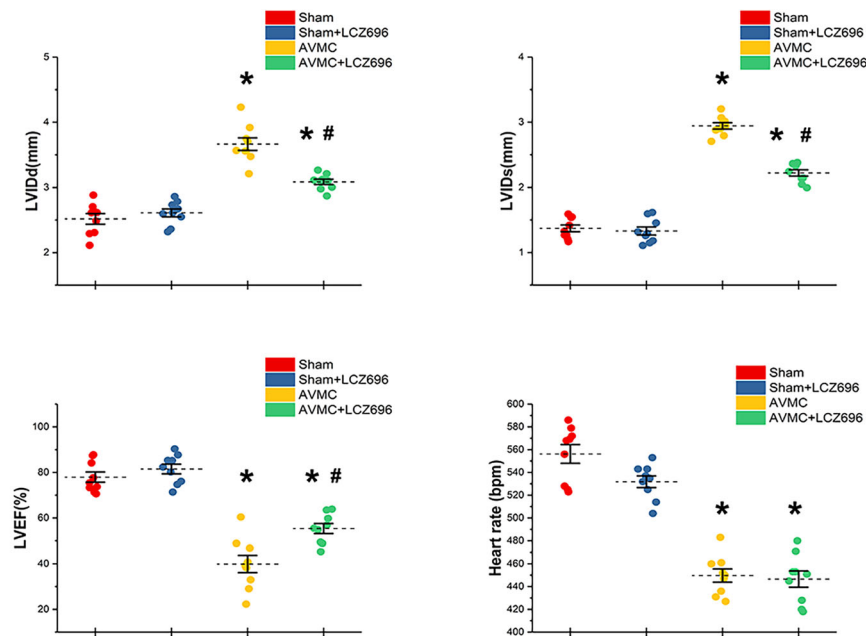
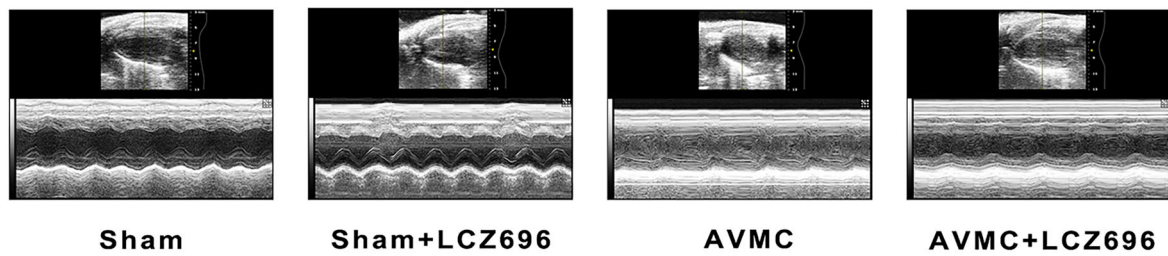
Mitochondria in cells was observed by MitoTracker Red and stained red (Figure 4A). Mdivi-1 decreased the expression of Drp1 in Sham + Mdivi-1 ( $0.27 \pm 0.25$  vs.  $1$  in Sham group,  $P < 0.05$ ) and CVB3 + Mdivi-1 groups ( $0.26 \pm 0.05$  vs.  $1.06 \pm 0.14$  in CVB3 group,  $P < 0.05$ ). The ratio of p-Drp1/Drp1 were  $1$ ,  $1.08 \pm 0.17$ ,  $1.93 \pm 0.26$ , and  $1.36 \pm 0.19$  in the Sham, Sham+ LCZ696, AVMC, and AVMC + LCZ696 groups. As same as AVMC mice treated with LCZ696, Mdivi-1 also reduced the p-Drp1/Drp1 in CVB3 injected HL-1 (Figure 4B). Increasing apoptosis cells were showed in the CVB3 group, and it attenuated by Mdivi-1 (Figure 4C), which the ratio of c-caspase-3/caspase-3 supported ( $7.67 \pm 1.36$  vs.  $2.77 \pm 0.95$ ,  $P < 0.05$ ) (Figure 4D). And the ratio in the Sham and Sham + Mdivi-1 groups were similar ( $P > 0.05$ ). The c-IL-1 $\beta$  and IL-6 were higher in the CVB3 group than the CVB3 + Mdivi-1 group and the Sham group (c-IL-1 $\beta$ : 1.43-fold and 1.64-fold; IL-6: 1.89-fold and 3.69-fold, respectively,  $P < 0.05$ ), which was no statistical significance between the Sham and Sham + Mdivi-1 group ( $P > 0.05$ ) (Figure 4D).

### Drp1 blocks the protection of cardiac function and survival of LCZ696

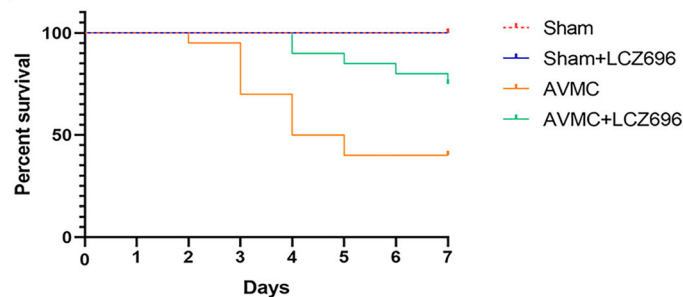
The HR in the AVMC, AVMC + AAV, AVMC + LCZ696, and AVMC + LCZ696 + AAV groups were  $403.44 \pm 18.15$ ,  $407.22 \pm 18.46$ ,  $413.22 \pm 21.27$ , and  $415.33 \pm 24.21$  bpm ( $P > 0.05$ ) (Figure 5A). The LVIDd, LVIDs, and LVEF in the AVMC, AVMC + AAV, AVMC + LCZ696, and AVMC + LCZ696 + AAV groups were  $3.70 \pm 0.37$ ,  $4.20 \pm 0.27^*$ ,  $2.83 \pm 0.25\%^*$ ,  $3.69 \pm 0.26\%^*$  and  $2.89 \pm 0.26$ ,  $3.51 \pm 0.21^*$ ,  $2.01 \pm 0.34\%^*$ ,  $2.89 \pm 0.18$  mm<sup>#</sup> and  $44.52 \pm 6.84\%$ ,  $34.78 \pm 4.67\%^*$ ,  $57.56 \pm 10.87\%^*$  and  $44.29 \pm 7.18\%^*$  (\* vs. AVMC,  $P < 0.05$ ; # vs. AVMC + AAV,  $P < 0.05$ ; & vs. AVMC + LCZ696,  $P < 0.05$ ) (Figure 5A). The survival rate was 45% in the AVMC group, 35% in the AVMC + AAV group, 65% in the AVMC + LCZ696 group, and 50% in the AVMC+LCZ696 + AAV group (Figure 5B).

**Figure 1** Effect of LCZ696 on cardiac function and survival rate (A) Typical M-mode echocardiograms of the long-axis midventricular view and HR, LVIDd, LVIDs, and LVEF ( $n = 9$  in each group). (B) The survival rate was measured every day until d7 ( $n = 20$  in each group). Results were presented as the mean  $\pm$  SD. \* $P < 0.05$  vs. Sham group; # $P < 0.05$  vs. AVMC group.

(A)



(B)



### Drp1 overexpression increased myocardial mitochondrial fission after LCZ696 treatment

The green fluorescent showed the successful injected of AAV with GFP (Figure 5C), and Figure 6B showed the up-regulated of Drp1 in the AVMC + AAV and AVMC + LCZ + AAV groups

(3.38-fold and 3.56-fold vs. AVMC group,  $P < 0.05$ ). The p-Drp1/Drp1 in AVMC, AVMC + AAV, AVMC + LCZ696, and AVMC + LCZ696 + AAV was 1,  $1.17 \pm 0.19$ ,  $0.42 \pm 0.09$ \*#, and  $0.54 \pm 0.12$ \*#, respectively (\* vs. AVMC,  $P < 0.05$ ; # vs. AVMC + AAV,  $P < 0.05$ ) (Figure 6B), which the IHC supported (Figure 6C). Smaller mitochondria were shown in AVMC, and



**Figure 2** Effect of LCZ696 on anti-inflammation and anti-apoptosis. (A) Cardiac inflammation revealed by HE staining (magnification: 40× and 100×). (B) IHC of IL-6 in each group (magnification: 200×). (C) TUNEL staining in myocardial tissue of each group (magnification: 200×). (D) The absolute intensity ratio of pro-inflammatory cytokines and c-caspase-3/caspase-3 ( $n = 6$  in each group). Results were presented as the mean  $\pm$  SD. \* $P < 0.05$  vs. Sham group; # $P < 0.05$  vs. AVMC group.

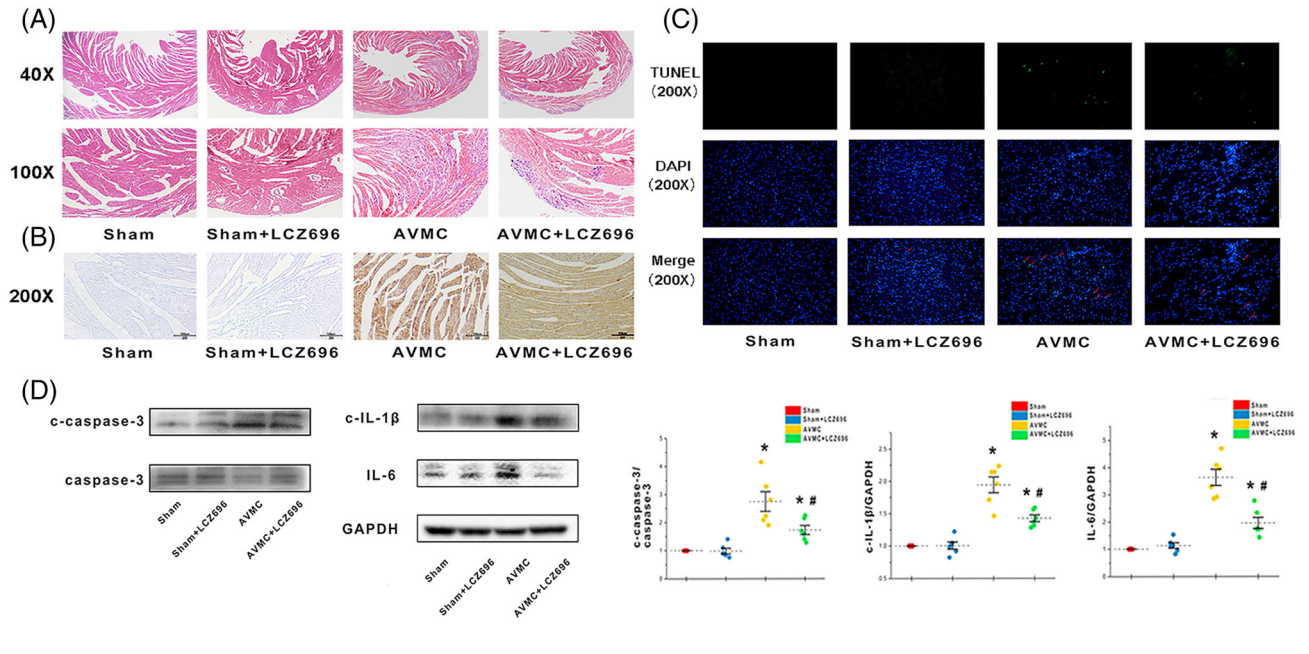


**Figure 3** Effect of LCZ696 on mitochondrial fission. (A) The morphology and structure of mitochondria in the myocardium of each group were detected by transmission electron microscopy (magnification: 15 000× and 150 000×). (B) The absolute intensity ratio of p-Drp1/Drp1 and Drp1/GAPDH ( $n = 6$  in each group). (C) IHC of p-Drp1 in each group (magnification: 100×). Results were presented as the mean  $\pm$  SD. \* $P < 0.05$  vs. Sham group; # $P < 0.05$  vs. AVMC group.

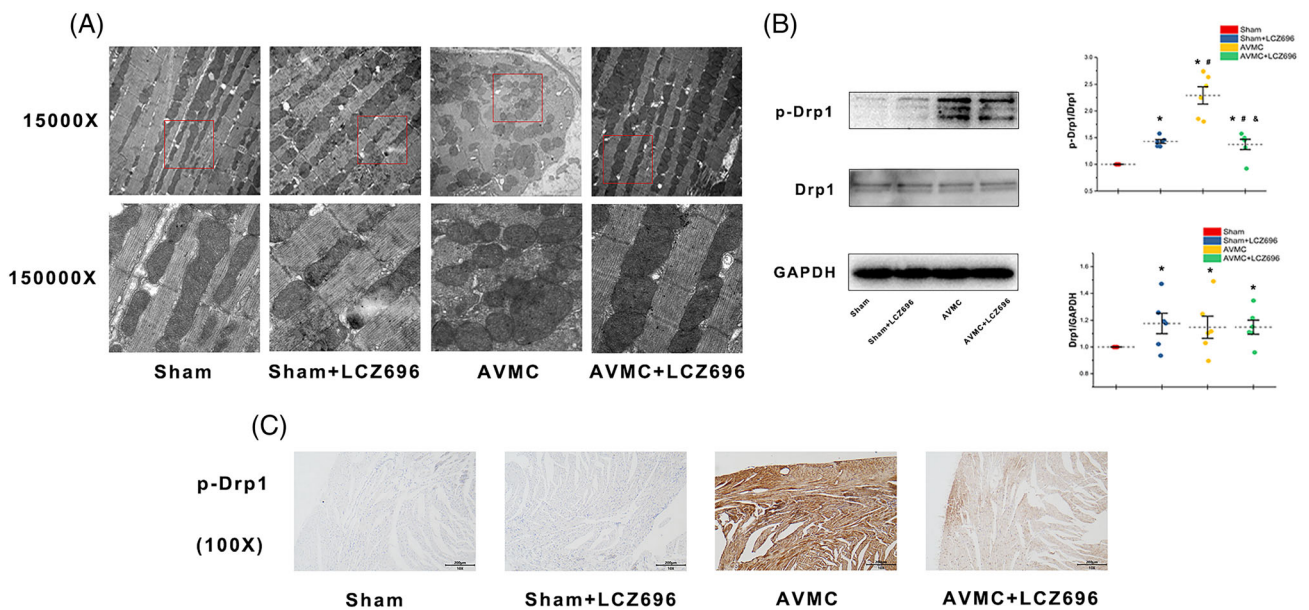


**Figure 4** Effect of Mdivi-1 on mitochondrial fission, anti-inflammation, and anti-apoptosis. (A) Mitochondria were stained with MitoTracker Red (magnification: 200×). (B) The absolute intensity ratio of p-Drp1/Drp1 and Drp1/GAPDH ( $n = 6$  in each group). (C) Hoechst staining in CVB3 induced HL-1 of each group. (D) The absolute intensity ratio of IL-6, c-IL-1 $\beta$ , and c-caspase-3/caspase-3 ( $n = 6$  in each group). Results were presented as the mean  $\pm$  SD. \* $P < 0.05$  vs. Sham group; # $P < 0.05$  vs. CVB3 group.

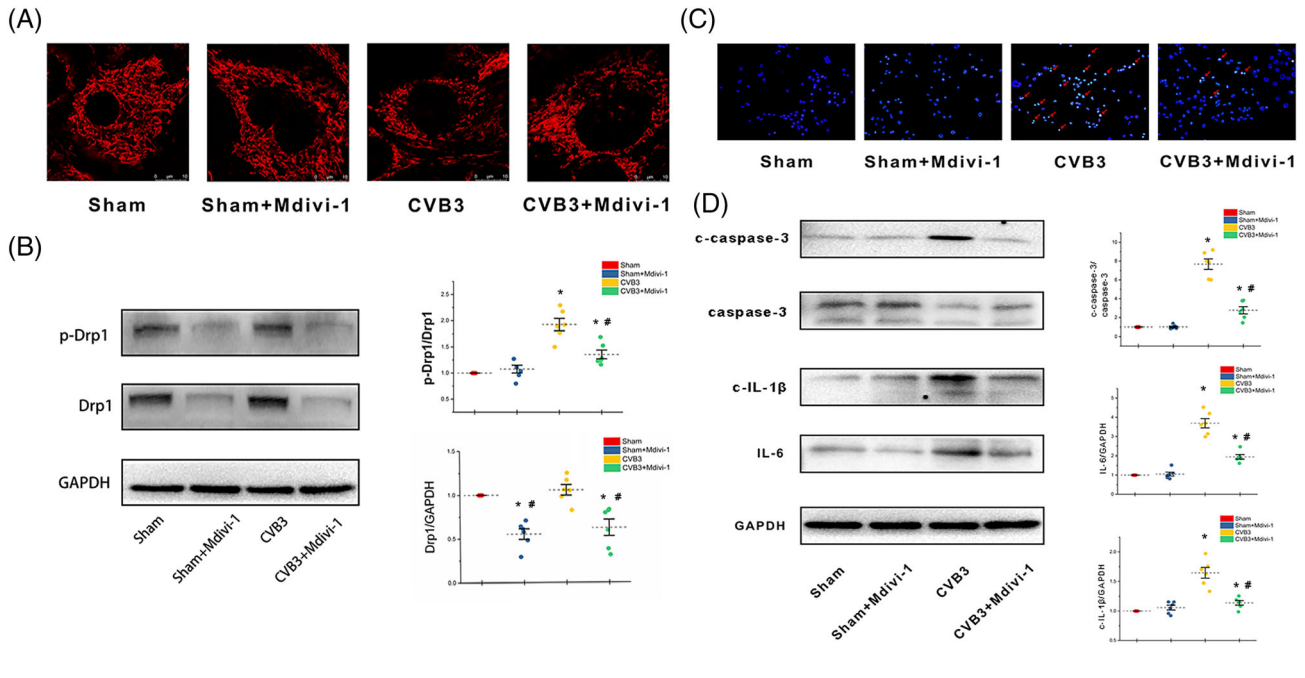


**Figure 5** Effect of Drp1 overexpression on cardiac function and survival rate. (A) Typical M-mode echocardiograms of the long-axis midventricular view, HR and LVIDd, LVIDs, and LVEF ( $n = 9$  in each group). (B) The survival rate was measured every day until d7 ( $n = 20$  in each group). (C) IF of the GFP contained by AAV in the AVMC + AAV and AVMC + LCZ696 + AAV group (magnification: 200×). Results were presented as the mean  $\pm$  SD. \* $P < 0.05$  vs. AVMC group; # $P < 0.05$  vs. AVMC + AAV group; & $P < 0.05$  vs. AVMC + LCZ696 group.

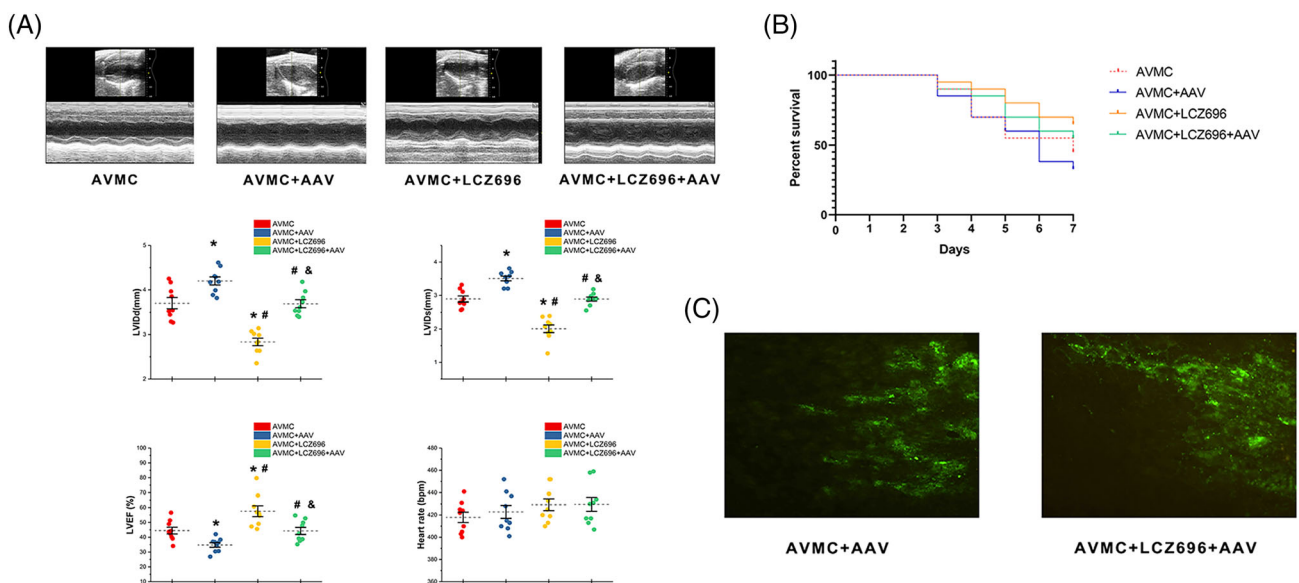
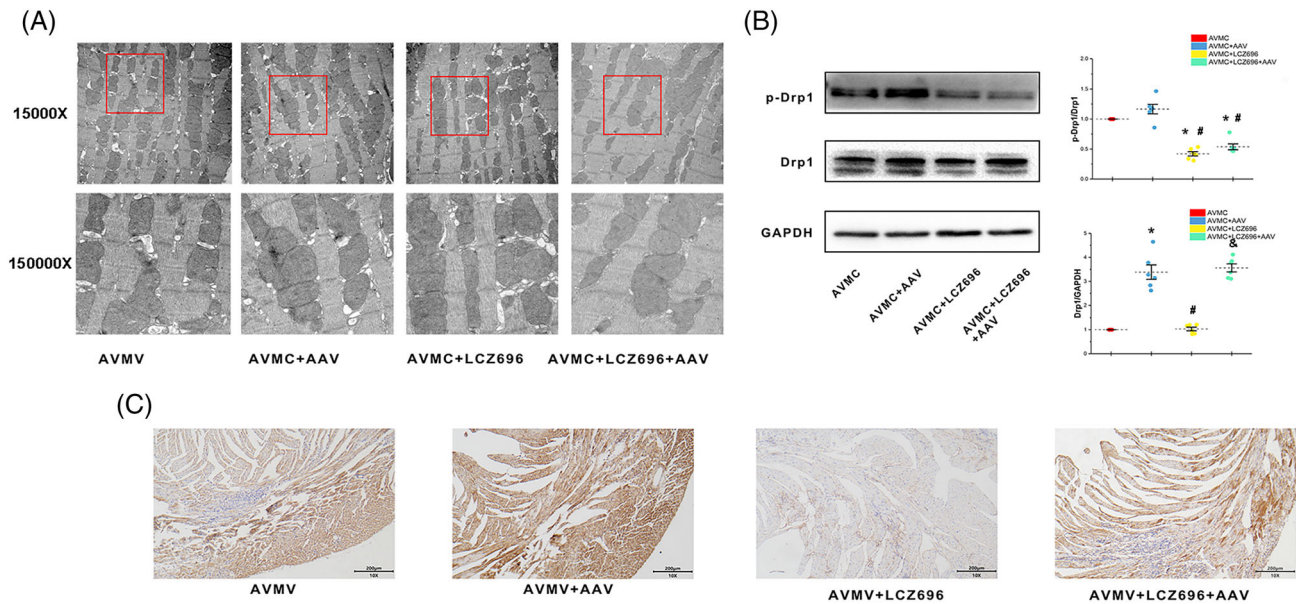


**Figure 6** Effect of Drp1 overexpression on mitochondria. (A) The morphology and structure of mitochondria in the myocardium of each group were detected by transmission electron microscopy (magnification: 15 000× and 150 000×). (B) The absolute intensity ratio of p-Drp1/Drp1 ( $n = 6$  in each group). (C) IHC of p-Drp1 in each group (magnification: 100×). Results were presented as the mean  $\pm$  SD. \* $P < 0.05$  vs. AVMC group; # $P < 0.05$  vs. AVMC + AAV group; & $P < 0.05$  vs. AVMC + LCZ696 group. &# $P < 0.05$  vs. AVMC + LCZ696 + AAV group.



it was more pronounced in AVMC + AAV. Mitochondrial width was increased in the AVMC + LCZ696 and AVMC + LCZ696 + AAV groups compared with the AVMC and AVMC + AAV groups, respectively (Figure 6A).

### Drp1 overexpression worsens inflammation and apoptosis

Figure 7A showed the most inflammatory cells infiltration areas in the AVMC + AAV group, followed by the AVMC + AAV + LCZ696, AVMC, and AVMC + LCZ696 groups. The expression of IL-6 in all groups was consistent with the infiltration of inflammatory cells (Figure 7B). Figure 7D shows the expression of c-IL-1 $\beta$  and IL-6 higher in AVMC + AAV group than that in other groups (c-IL-1 $\beta$ : 1, 2.54  $\pm$  0.44\*, 0.79  $\pm$  0.09\*#, 1.03  $\pm$  0.14#&; IL-6: 1, 2.72  $\pm$  0.16\*, 0.72  $\pm$  0.08\*#, 1.07  $\pm$  0.22#& in AVMC, AVMC + AAV, AVMC + LCZ696, AVMC + LCZ696 + AAV; \* vs. AVMC,  $P < 0.05$ ; # vs. AVMC + AAV,  $P < 0.05$ ; & vs. AVMC + LCZ696,  $P < 0.05$ )

TUNEL staining showed the greatest number of apoptotic cells in AVMC + AAV group, followed by the AVMC, AVMC + LCZ696 + AAV, and then AVMC + LCZ696 groups (Figure 7C). The c-caspase-3/caspase-3 ratio in the AVMC + LCZ696 + AAV group (0.93  $\pm$  0.13) was not significant compared with that in the AVMC group (1,  $P > 0.05$ ), which was higher than in the AVMC + LCZ696 group (0.56  $\pm$  0.18,

$P < 0.05$ ) but lower than in the AVMC + AAV group (4.69  $\pm$  0.29,  $P < 0.05$ ) (Figure 7D).

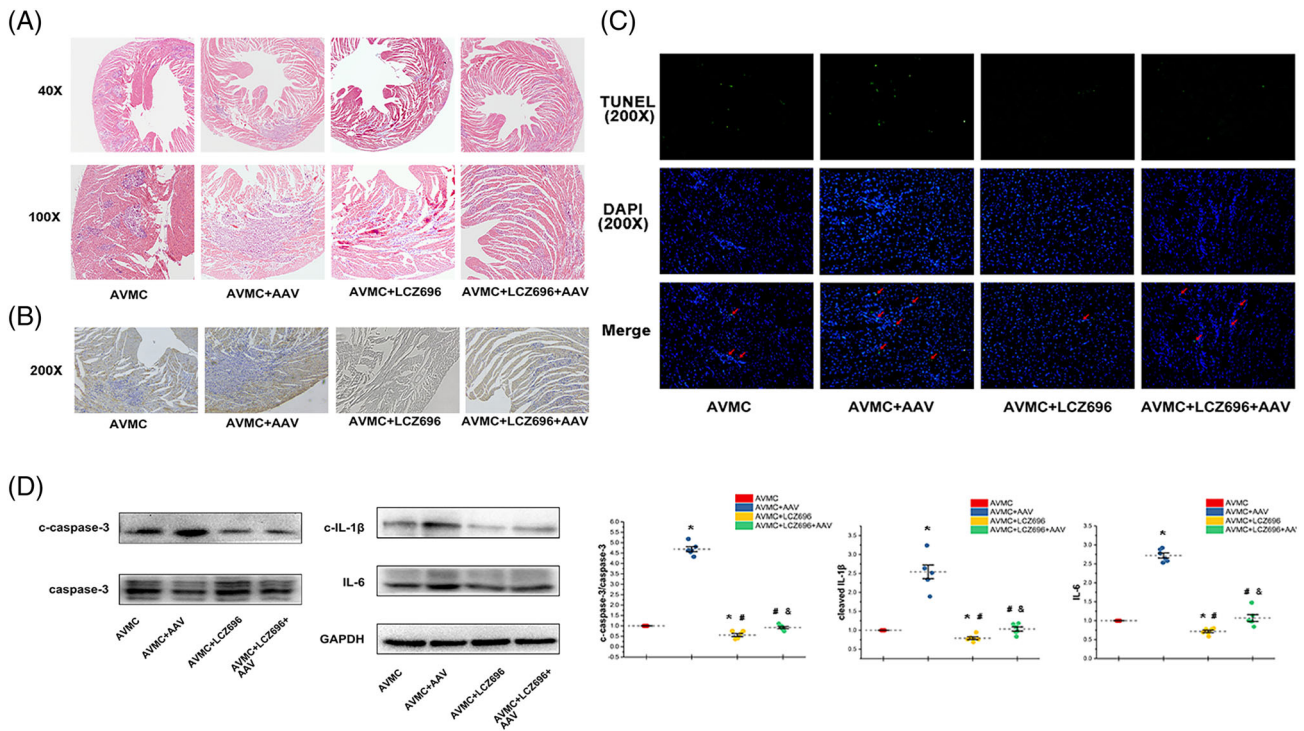
## Discussion

This is the first study to investigate the effects of LCZ696 in AVMC and to explore its mechanism. In this study, we confirmed that 7 days of LCZ696 treatment has a protective effect in AVMC, and Drp1 may play an important role.

LCZ696 has been shown to have a higher therapeutic value than enalapril in HFrEF. Suematsu *et al.* reported that LCZ696 offered a superior effect than valsartan in improving LVEF in chronic kidney disease rat.<sup>24</sup> Trivedi *et al.* found LCZ696 provided a significant and sustained improvement in LVEF in myocardial ischaemia/reperfusion rat.<sup>25</sup> They also identified the involvement of LCZ696 in improving cardiac remodelling. However, there is no study reported on the similar result of LCZ696 in AVMC, which our present study indicated that LCZ696 increased the survival and LVEF of AVMC mice. Our previous study confirmed that normal mice have a higher HR than AVMC mice,<sup>26</sup> but we did not observe the effect of LCZ696 in improving HR. Our research proved the anti-inflammatory and anti-apoptotic of LCZ696 in AVMC, which have found in different cardiovascular diseases. Research in mice following pressure unloading demonstrated blunted inflammatory infiltration in the heart, LCZ696 de-



**Figure 7** Effect of Drp1 overexpression on inflammation and apoptosis. (A) Cardiac inflammation revealed by HE staining (magnification: 40× and 100×). (B) IHC of IL-6 (magnification: 200×). (C) TUNEL staining in myocardial tissue (magnification: 200×). (D) The ratio of IL-6, c-IL-1 $\beta$ , and c-caspase-3/caspase-3. \* $P < 0.05$  vs. AVMC group; # $P < 0.05$  vs. AVMC + AAV group; & $P < 0.05$  vs. AVMC + LCZ696 group.



creased mRNA level of IL-1 $\beta$  and TNF- $\alpha$  and inhibited NLRP3 activity.<sup>27</sup> Ge *et al.* and Xia *et al.* found that LCZ696 attenuates inflammation, apoptosis, and oxidative stress in DCM.<sup>9,28</sup> In our study, apoptosis and inflammation levels were reduced by LCZ696, demonstrated by a depressed c-caspase-3/caspase-3 ratio, fewer dead cells, lower levels of pro-inflammatory cytokines, and less infiltration of inflammatory cells, which extend the cardioprotective effect of LCZ696 to CVB3-induced AVMC. However, its mechanism in AVMC remains controversial.

New evidence suggests that mitochondrial fission is critical in a variety of physiological and pathological processes, including cell division, apoptosis, and necrosis.<sup>29,30</sup> Drp1, a key protein in the mitochondrial division, is considered a possible key site for the treatment of multiple diseases.<sup>31</sup> Lin *et al.* and Hui Shi *et al.* found that Drp1-mediated mitochondrial dysfunction was associated with the onset of inflammation as well as apoptosis in AVMC, which could be rescued after inhibiting Drp1 Ser616 phosphorylation.<sup>19,20</sup> In line with the above research, we found a remarkable increase in the phosphorylation level of Drp1 Ser616, which led to increased mitochondrial fission in AVMC compared with the Sham group. Their findings were replicated *in vitro* experiments. Interestingly, Xia *et al.* suggested that the protective effect of LCZ696 against DCM may be related to the regulation of

mitochondrial fission mediated by Drp1 phosphorylation.<sup>9</sup> However, the mechanism of LCZ696 in AMVC has never been reported. Therefore, in conjunction with the strong relationship between mitochondrial division and multiple cardiovascular diseases, we sought to explain our finding that LCZ696 can also regulate Drp1-mediated mitochondrial fission in AVMC. Our results confirmed the suspicion that LCZ696 down-regulates mitochondrial fission by inhibiting Drp1 Ser616 phosphorylation but has no effect on Drp1 expression. Next, to verify that the improved cardiac function and anti-inflammatory and anti-apoptotic effects of LCZ696 in AVMC were achieved by regulating Drp1, we used AAV9 to up-regulate the expression of Drp1. As a result, we found that overexpression of Drp1 counteracted part of the protective effect of LCZ696.

However, treatment of AVMC is still scarce because the progress remains unclear. A critical question that intrigues us is that the patient seems to be selected for developing myocarditis. Up to 90% of individuals will be infected with one or more cardiophilic viruses during their lifetime, but few of them will develop clinical signs of AVMC.<sup>3</sup> In animals, evidence demonstrated the relation between AVMC to genetic. Different strains of mice show completely different disease progression and prognosis after infection with viruses injected. A.BY/SnJ and SWR/J exhibit persistent cardiac in-

inflammation accompanied by the prolonged presence of viral RNA within the cardiomyocyte, whereas C57BL/6J and DBA/1J show strong resistance to the virus.<sup>32</sup> In human studies, the occurrence of DCM and the progression of AVMC to DCM have been shown to be associated with individual susceptibility; unfortunately, there is no clear evidence to confirm a genetic relationship with AVMC.<sup>3</sup> Such results seem to indicate that genetic background seems to be an important direction for future research and treatment of AVMC. However, because there is much evidence for the importance of genetic susceptibility in AVMC, future studies could focus on understanding the potential relationship between genetic susceptibility and inflammation and immunity in AVMC.

In conclusion, we confirmed that LCZ696 ultimately enhanced cardiac function and resistance to inflammation and apoptosis in AVMC mice by inhibiting phosphorylation of the Drp1 Ser616 site.

## References

- McDonagh TA, Metra M, Adamo M, Gardner RS, Baumach A, Böhm M, Burri H, Butler J, Čelutkienė J, Chioncel O, Cleland JGF, Coats AJS, Crespo-Leiro MG, Farmakis D, Gilard M, Heymans S, Hoes AW, Jaarsma T, Jankowska EA, Lainscak M, Lam CSP, Lyon AR, McMurray JJV, Mebazaa A, Mindham R, Muneretto C, Francesco Piepoli M, Price S, Rosano GMC, Ruschitzka F, Kathrine Skibelund A, ESC Scientific Document Group, de Boer RA, Christian Schulze P, Abdelhamid M, Aboyans V, Adamopoulos S, Anker SD, Arbelo E, Asteggiano R, Bauersachs J, Bayes-Genis A, Borger MA, Budts W, Cikes M, Damman K, Delgado V, Dendale P, Dilaveris P, Drexler H, Ezekowitz J, Falk V, Fauchier L, Filippatos G, Fraser A, Frey N, Gale CP, Gustafsson F, Harris J, Iung B, Janssens S, Jessup M, Konradi A, Kotecha D, Lambrinou E, Lancellotti P, Landmesser U, Leclercq C, Lewis BS, Leyva F, Linhart A, Løchen ML, Lund LH, Mancini D, Masip J, Milicic D, Mueller C, Nef H, Nielsen JC, Neubeck L, Noutsias M, Petersen SE, Sonia Petronio A, Ponikowski P, Prescott E, Rakisheva A, Richter DJ, Schlyakhto E, Seferovic P, Senni M, Sitges M, Sousa-Uva M, Tocchetti CG, Touyz RM, Tschoepe C, Waltenberger J, Adamo M, Baumach A, Böhm M, Burri H, Čelutkienė J, Chioncel O, Cleland JGF, Coats AJS, Crespo-Leiro MG, Farmakis D, Gardner RS, Gilard M, Heymans S, Hoes AW, Jaarsma T, Jankowska EA, Lainscak M, Lam CSP, Lyon AR, McMurray JJV, Mebazaa A, Mindham R, Muneretto C, Piepoli MF, Price S, Rosano GMC, Ruschitzka F, Skibelund AK. 2021 ESC guidelines for the diagnosis and treatment of acute and chronic heart failure. *Eur Heart J*. 2021; **42**: 3599–3726.
- Ammirati E, Frigerio M, Adler ED, Basso C, Birnie DH, Brambatti M, Friedrich MG, Klingel K, Lehtonen J, Moslehi JJ, Pedrotti P, Rimoldi OE, Schultheiss HP, Tschöpe C, Cooper LT Jr, Camici PG. Management of acute myocarditis and chronic inflammatory cardiomyopathy: An expert consensus document. *Circ Heart Fail*. 2020; **13**: e007405.
- Dennert R, Crijns HJ, Heymans S. Acute viral myocarditis. *Eur Heart J*. 2008; **29**: 2073–2082.
- Ammirati E, Cipriani M, Moro C, Raineri C, Pini D, Sormani P, Mantovani R, Varrenti M, Pedrotti P, Conca C, Mafri A, Grosu A, Briguglia D, Guglielmetto S, Perego GB, Colombo S, Caico SI, Giannattasio C, Maestroni A, Carubelli V, Metra M, Lombardi C, Campodonico J, Agostoni P, Peretto G, Scelsi L, Turco A, di Tano G, Campana C, Belloni A, Morandi F, Mortara A, Cirò A, Senni M, Gavazzi A, Frigerio M, Oliva F, Camici PG, on behalf of the Registro Lombardo delle Miocarditi. Clinical presentation and outcome in a contemporary cohort of patients with acute myocarditis: Multicenter Lombardy registry. *Circulation*. 2018; **138**: 1088–1099.
- Tschöpe C, Ammirati E, Bozkurt B, Caforio ALP, Cooper LT, Felix SB, Hare JM, Heidecker B, Heymans S, Hübner N, Kelle S, Klingel K, Maatz H, Parwani AS, Spillmann F, Starling RC, Tsutsui H, Seferovic P, van Linthout S. Myocarditis and inflammatory cardiomyopathy: Current evidence and future directions. *Nat Rev Cardiol*. 2021; **18**: 169–193.
- Voors AA, Dorhout B, van der Meer P. The potential role of valsartan + AHU377 (LCZ696) in the treatment of heart failure. *Expert Opin Investig Drugs*. 2013; **22**: 1041–1047.
- Solomon SD, Claggett B, Desai AS, Packer M, Zile M, Swedberg K, Rouleau JL, Shi VC, Starling SC, Kozan Ö, Dukat A, Lefkowitz MP, McMurray J. Influence of ejection fraction on outcomes and efficacy of sacubitril/valsartan (LCZ696) in heart failure with reduced ejection fraction: The prospective comparison of ARNI with ACEI to determine impact on global mortality and morbidity in heart failure (PARADIGM-HF) trial. *Circ Heart Fail*. 2016 Mar [cited 2022 Feb 6];9(3). Available from: **9**: e002744.
- Suematsu Y, Miura S, Goto M, Matsuo Y, Arimura T, Kuwano T, Imaizumi S, Iwata A, Yahiro E, Saku K. LCZ696, an angiotensin receptor-neprilysin inhibitor, improves cardiac function with the attenuation of fibrosis in heart failure with reduced ejection fraction in streptozotocin-induced diabetic mice: LCZ696 improves cardiac function. *Eur J Heart Fail*. 2016; **18**: 386–393.
- Xia Y, Chen Z, Chen A, Fu M, Dong Z, Hu K, Yang X, Zou Y, Sun A, Qian J, Ge J. LCZ696 improves cardiac function via alleviating Drp1-mediated mitochondrial dysfunction in mice with doxorubicin-induced dilated cardiomyopathy. *J Mol Cell Cardiol*. 2017; **108**: 138–148.
- von Lueder TG, Wang BH, Kompa AR, Huang L, Webb R, Jordaan P, Atar D, Krum H. Angiotensin receptor Neprilysin inhibitor LCZ696 attenuates cardiac remodeling and dysfunction after myocardial infarction by reducing cardiac fibrosis and hypertrophy. *Circ Heart Fail*. 2015; **8**: 71–78.
- Sabbah HN, Zhang K, Gupta RC, Xu J, Singh-Gupta V. Effects of

## Conflict of interest

All authors declare that they have no conflict of interest.

## Funding

This study was supported by grants from the National Natural Science Foundation of China (Grant No. 81870281), the Natural Science Foundation of Zhejiang Province (Grant No. LQ19H020005), and the Wenzhou Municipal Science and Technology Bureau (Grant No. Y20210137). The funders had no role in study design, data collection and analysis, decision to publish, or preparation of the manuscript.

- angiotensin-neprilysin inhibition in canines with experimentally induced cardiorenal syndrome. *J Card Fail.* 2020; **26**: 987–997.
12. Li X, Braza J, Mende U, Choudhary G, Zhang P. Cardioprotective effects of early intervention with sacubitril/valsartan on pressure overloaded rat hearts. *Sci Rep.* 2021; **11**: 16542.
  13. Dorn GW, Vega RB, Kelly DP. Mitochondrial biogenesis and dynamics in the developing and diseased heart. *Genes Dev.* 2015; **29**: 1981–1991.
  14. Vásquez-Trincado C, García-Carvajal I, Pennanen C, Parra V, Hill JA, Rothmel BA, Lavandero S. Mitochondrial dynamics, mitophagy and cardiovascular disease: Mitochondria and cardiovascular disease. *J Physiol.* 2016; **594**: 509–525.
  15. Shirakabe A, Zhai P, Ikeda Y, Saito T, Maejima Y, Hsu C-P, Nomura M, Egashira K, Levine B, Sadoshima J. Drp1-dependent mitochondrial autophagy plays a protective role against pressure overload-induced mitochondrial dysfunction and heart failure. *Circulation.* 2016; **133**: 1249–1263.
  16. Wang J-X, Jiao J-Q, Li Q, Long B, Wang K, Liu J-P, Li YR, Li PF. miR-499 regulates mitochondrial dynamics by targeting calcineurin and dynamin-related protein-1. *Nat Med.* 2011; **17**: 71–78.
  17. Ong S-B, Subrayan S, Lim SY, Yellon DM, Davidson SM, Hausenloy DJ. Inhibiting mitochondrial fission protects the heart against ischemia/reperfusion injury. *Circulation.* 2010; **121**: 2012–2022.
  18. Cereghetti GM, Stangherlin A, de Brito OM, Chang CR, Blackstone C, Bernardi P, Scorrano L. Dephosphorylation by calcineurin regulates translocation of Drp1 to mitochondria. *Proc Natl Acad Sci.* 2008; **105**: 15803–15808.
  19. Shi H, Yu Y, Liu X, Yu Y, Li M, Wang Y, Zou Y, Chen R, Ge J. Inhibition of calpain reduces cell apoptosis by suppressing mitochondrial fission in acute viral myocarditis. *Cell Biol Toxicol.* 2021; **38**: 487–504.
  20. Lin L, Zhang M, Yan R, Shan H, Diao J, Wei J. Inhibition of Drp1 attenuates mitochondrial damage and myocardial injury in coxsackievirus B3 induced myocarditis. *Biochem Biophys Res Commun.* 2017; **484**: 550–556.
  21. Zacchigna S, Paldino A, Falcão-Pires I, Daskalopoulos EP, Dal Ferro M, Vodret S, Lesizza P, Cannatà A, Miranda-Silva D, Lourenço AP, Pinamonti B, Sinagra G, Weinberger F, Eschenhagen T, Carrier L, Kehat I, Tocchetti CG, Russo M, Ghigo A, Cimino J, Hirsch E, Dawson D, Ciccarelli M, Olivetti M, Linke WA, Cuijpers I, Heymans S, Hamdani N, de Boer M, Duncker DJ, Kuster D, van der Velden J, Beauloye C, Bertrand L, Mayr M, Giacca M, Leuschner F, Backs J, Thum T. Towards standardization of echocardiography for the evaluation of left ventricular function in adult rodents: A position paper of the ESC working group on myocardial function. *Cardiovasc Res.* 2021; **117**: 43–59.
  22. Yue-Chun L, Gu X-H, Li-Sha G, Zhou D-P, Xing C, Guo X-L, Pan LL, Song SY, Yu LL, Chen GY, Lin JF, Chu MP. Vagus nerve plays a pivotal role in CD4+ T cell differentiation during CVB3-induced murine acute myocarditis. *Virulence.* 2021; **12**: 360–376.
  23. Cheng Z, Li-Sha G, Jing-Lin Z, Wen-Wu Z, Xue-Si C, Xing-Xing C, Yue-Chun L. Protective role of the cholinergic anti-inflammatory pathway in a mouse model of viral myocarditis. *PLoS ONE.* 2014; **9**: e112719.
  24. Suematsu Y, Jing W, Nunes A, Kashyap ML, Khazaeli M, Vaziri ND, Moradi H. LCZ696 (sacubitril/valsartan), an angiotensin-receptor neprilysin inhibitor, attenuates cardiac hypertrophy, fibrosis, and vasculopathy in a rat model of chronic kidney disease. *J Card Fail.* 2018; **24**: 266–275.
  25. Trivedi RK, Polhemus DJ, Li Z, Yoo D, Koiwaya H, Scarborough A, Goodchild TT, Lefer DJ. Combined angiotensin receptor–neprilysin inhibitors improve cardiac and vascular function via increased NO bioavailability in heart failure. *JAHA.* 2018; **7**.
  26. Yue-Chun L, Teng Z, Na-Dan Z, Li-Sha G, Qin L, Xue-Qiang G, Jia-Feng L. Comparison of effects of ivabradine versus carvedilol in murine model with the coxsackievirus B3-induced viral myocarditis. *PLoS ONE.* 2012; **7**: e39394.
  27. Li X, Zhu Q, Wang Q, Zhang Q, Zheng Y, Wang L, Jin Q. Protection of sacubitril/valsartan against pathological cardiac remodeling by inhibiting the NLRP3 inflammasome after relief of pressure overload in mice. *Cardiovasc Drugs Ther.* 2020; **34**: 629–640.
  28. Ge Q, Zhao L, Ren X-M, Ye P, Hu Z-Y. LCZ696, an angiotensin receptor-neprilysin inhibitor, ameliorates diabetic cardiomyopathy by inhibiting inflammation, oxidative stress and apoptosis. *Exp Biol Med (Maywood).* 2019; **244**: 1028–1039.
  29. Wang Y, Subramanian M, Yurdagul A, Barbosa-Lorenzi VC, Cai B, de Juan-Sanz J, Ryan TA, Nomura M, Maxfield FR, Tabas I. Mitochondrial fission promotes the continued clearance of apoptotic cells by macrophages. *Cell.* 2017; **171**: 331–345.e22.
  30. Quirós PM, Langer T, López-Otín C. New roles for mitochondrial proteases in health, ageing and disease. *Nat Rev Mol Cell Biol.* 2015; **16**: 345–359.
  31. Tong M, Zablocki D, Sadoshima J. The role of Drp1 in mitophagy and cell death in the heart. *J Mol Cell Cardiol.* 2020; **142**: 138–145.
  32. Chow LH, Gauntt CJ, McManus BM. Differential effects of myocarditic variants of coxsackievirus B3 in inbred mice. A pathologic characterization of heart tissue damage. *Lab Invest.* 1991; **64**: 55–64.